nature physics

SUPPLEMENTARY INFORMATION

https://doi.org/10.1038/s41567-020-0917-6

In the format provided by the authors and unedited.

Repulsive photons in a quantum nonlinear medium

Sergio H. Cantu[1,2,5], Aditya V. Venkatramani[3,5], Wenchao Xu[1,2], Leo Zhou[3], Brana Jelenković[4], Mikhail D. Lukin[3] ✉ and Vladan Vuletić[1,2] ✉

[1]Department of Physics, Massachusetts Institute of Technology, Cambridge, MA, USA. [2]Research Laboratory of Electronics, Massachusetts Institute of Technology, Cambridge, MA, USA. [3]Department of Physics, Harvard University, Cambridge, MA, USA. [4]Photonics Center, Institute of Physics, University of Belgrade, Belgrade, Serbia. [5]These authors contributed equally to this work: Sergio H. Cantu, Aditya V. Venkatramani. ✉ e-mail: lukin@physics.harvard.edu; vuletic@mit.edu

Supplementary information to: Repulsive photons in a quantum nonlinear medium

Sergio H. Cantu,[1,*] Aditya V. Venkatramani,[2,*] Wenchao Xu,[1] Leo Zhou,[2] Brana Jelenković,[3] Mikhail D. Lukin,[2] and Vladan Vuletić[1]

[1] *Department of Physics and Research Laboratory of Electronics, Massachusetts Institute of Technology, Cambridge, Massachusetts 02139, USA*
[2] *Department of Physics, Harvard University, Cambridge, Massachusetts 02138, USA*
[3] *Photonics Center, Institute of Physics, University of Belgrade, Serbia*

Contents

I. METHODS

A. Atom preparation

^{87}Rb atoms are cooled in a 3D magneto-optical trap (MOT) and loaded into a far-off detuned 1064 nm crossed dipole trap with an opening angle of 32°. This results in a cigar-shaped atomic cloud with dimensions root-mean-squared (RMS) axial width of 32 μm and radial width of 8 μm with optical depth (OD) of ~ 30. The cloud is cooled to 50 μK using polarization gradient cooling to reduce Doppler broadening of atomic transitions.

We apply a magnetic field of 15.5 Gauss along the direction of propagation of the probe to set our quantization axis. The magnitude is chosen to separate the magnetic Zeeman levels sufficiently to minimize effects from other states. The atoms are optically pumped (Fig.1A) into the hyperfine (F) and Zeeman (m_F) sublevel $|g\rangle = |5S_{1/2}, F = 1, m_F = 1\rangle$. A weak probe field (≈ 1 ph μsec^{-1}) which is at 780 nm and σ_+-polarized, addresses $|g\rangle$ to the intermediate state $|p\rangle = |5P_{3/2}, F = 2, m_F = 2\rangle$. The probe is coupled to the Rydberg state $|r\rangle = |73S_{1/2}, m_J = 1/2\rangle$ by a counter σ_- polarized propagating control field at 479 nm. The probe field is also coupled to a non-interacting hyperfine ground state $|f\rangle = |5S_{1/2}, F = 2, m_F = 2\rangle$, by a π-polarized control field at 780 nm applied perpendicularly. At single-photon detuning of $\Delta/2\pi = -16$ MHz, and our quantization field of 15.5 Gauss, the control laser coupling $|f\rangle$ and $|e\rangle$ also couples $|f\rangle$ and $|5P_{3/2}, F = 2, m_F = 1\rangle$ from residual σ_--polarization of $\approx 1\%$ compared to the expected π-polarization. δ_f in the numerics is corrected for the stark shift arising from this spurious coupling, which shifts δ_f by ≈ 300 KHz for parameters in Fig.3 of the main text.

The Rydberg state $|r\rangle$ strongly interacts with a Van-der Waals interaction $V(z) = C_6/z^6$, where $C_6/\hbar = 2\pi \times$ 1.8 THz μm^6. The probe beam is focused to a waist of $\omega \sim 4.5$ μm, smaller than the blockade radius of $\sim$10 μm, resulting in an effective 1D system for the propagation of the probe polariton. We send a probe pulse for 6 μs repeating every 40 μs. The dipole trap is turned off during probing to prevent anti-trapping atoms in the Rydberg state and non-homogeneous AC stark shifts of the states. We repeat this 1500 times every 1.5 seconds before we have to reload and cool atoms into the dipole trap again.

---

*These authors contributed equally to this work

B. Correlation measurements

To study the correlations between photons after they pass through the atomic gas (Fig.1A), we split the beam into three paths. This allows us to measure two and three photon correlation function g^2 and g^3. Suppose detectors 1,2,3 detect n_1, n_2, n_3 photons at times t_1, t_2, t_3, then $g^2(t_2 - t_1) = \frac{\langle n_1(t_1) n_2(t_2)\rangle}{\langle n_1(t_1)\rangle\langle n_2(t_2)\rangle}$, where $\langle\rangle$ denotes averages over multiple experimental repeats. g^2 can similarly be defined over all combinations of pairs of detectors. $g^3(t_2 - t_1, t_3 - t_1) = \frac{\langle n_1(t_1) n_2(t_2) n_3(t_3)\rangle}{\langle n_1(t_1)\rangle\langle n_2(t_2)\rangle\langle n_3(t_3)\rangle}$.

To measure the conditional phase of the photons, we send a local oscillator (LO) co-propagating alongside the the probe. The LO is detuned 80 MHz away from the probe and propagates with orthogonal polarization to suppress photon scattering from the atomic cloud. The LO is then mixed into one of the detectors (d_1) using a 8:92 pellicle beamsplitter. We perform a heterodyne measurement to obtain the phase of the probe beam as a function of time t_1. This phase can be conditioned on detecting a photon on either one of the other detectors at time t_2 to give us the conditional phase $\phi^2(t_2 - t_1)$.

These correlation functions can be related to the two-photon wave function. Let us denote $E(z)$ as the probability amplitude of having a photon at position z. This can be extended to two photons by the probability amplitude $EE(z_2 - z_1)$, which would correspond to having two photons at positions z_1 and z_2. Then $g^2(t_2 - t_1) = \left|\frac{EE(c(t_2-t_1))}{E(ct_1)E(ct_2)}\right|^2$, and $\phi^2(t_2 - t_1) = \mathrm{Arg}\left(\frac{EE(c(t_2-t_1))}{E(ct_1)E(ct_2)}\right)$. Measuring g^2 and ϕ^2 directly gives us information about the two photon amplitude. This definition can be analogously extended to g^3 as well.

II. A TWO-COMPONENT EFFECTIVE EQUATION GOVERNING POLARITON DYNAMICS

In this section, we derive the effective theoretical description of polariton dynamics that we experimentally observe. We start with the two-body equations of motion that has 16 components, and perform a series of approximations and simplication that culminates in the two-component Schrödinger-like equation (1) in the main text.

As the experiments are conducted in the regime where the waist of the probe beam is much smaller than the Rydberg blockade radius in the atomic medium, we assume the dynamics of quasi-particle excitations are confined to one dimension to good approximation. In the context of the 4-level scheme shown in Figure 1B, let us denote $\hat{\mathcal{E}}^\dagger(z), \hat{\mathcal{P}}^\dagger(z), \hat{\mathcal{R}}^\dagger(z), \hat{\mathcal{F}}^\dagger(z)$ as the creation operator of a photon, an intermediate-state excitation $|p\rangle$, a Rydberg excitation $|r\rangle$, and an excitation in the non-interacting ground state $|f\rangle$, respectively, at position z. These operators satisfy the bosonic commutation relation $[\hat{\mathcal{E}}(z), \hat{\mathcal{E}}^\dagger(z')] = [\hat{\mathcal{P}}(z), \hat{\mathcal{P}}^\dagger(z')] = [\hat{\mathcal{R}}(z), \hat{\mathcal{R}}^\dagger(z')] = [\hat{\mathcal{F}}(z), \hat{\mathcal{F}}^\dagger(z')] = \delta(z - z')$.

Under the scheme shown in Fig. 1B, the Hamiltonian governing the system within the atomic medium is

$$\mathcal{H} = \mathcal{H}_0 + \mathcal{H}_{\text{int}}, \quad \text{where} \quad \mathcal{H}_0 = \int dz \begin{pmatrix} \hat{\mathcal{E}} \\ \hat{\mathcal{P}} \\ \hat{\mathcal{R}} \\ \hat{\mathcal{F}} \end{pmatrix}^\dagger \begin{pmatrix} -ic\partial_z & g/2 & 0 & 0 \\ g/2 & -\Delta & \Omega_r/2 & \Omega_f/2 \\ 0 & \Omega_r/2 & -\delta_r & 0 \\ 0 & \Omega_f/2 & 0 & -\delta_f \end{pmatrix} \begin{pmatrix} \hat{\mathcal{E}} \\ \hat{\mathcal{P}} \\ \hat{\mathcal{R}} \\ \hat{\mathcal{F}} \end{pmatrix} \tag{S1}$$

$$\text{and} \quad \mathcal{H}_{\text{int}} = \frac{1}{2} \iint dz dz' V(z - z') \hat{\mathcal{R}}^\dagger(z) \hat{\mathcal{R}}^\dagger(z') \hat{\mathcal{R}}(z') \hat{\mathcal{R}}(z) \tag{S2}$$

where g is the collective photon-atom coupling determined by the atomic density resonant atomic cross section. In our experimental regime of high optical depth OD $= 30$, g is larger than the other parameters in the Hamiltonian $\mathcal{H}_0$ by an of magnitude.

In the Heisenberg picture, the particle operators obey the following Heisenberg equations of motion:

$$i\partial_t \hat{\mathcal{E}} = -ic\partial_z \hat{\mathcal{E}} + \frac{g}{2}\hat{\mathcal{P}} \tag{S3}$$

$$i\partial_t \hat{\mathcal{P}} = -\Delta\hat{\mathcal{P}} + \frac{g}{2}\hat{\mathcal{E}} + \frac{\Omega_r}{2}\hat{\mathcal{R}} + \frac{\Omega_f}{2}\hat{\mathcal{F}} \tag{S4}$$

$$i\partial_t \hat{\mathcal{R}} = -\delta_c \hat{\mathcal{R}} + \frac{\Omega_r}{2}\hat{\mathcal{P}} + \int dz' V(z - z') \hat{\mathcal{R}}^\dagger(z') \hat{\mathcal{R}}(z') \hat{\mathcal{R}}(z) \tag{S5}$$

$$i\partial_t \hat{\mathcal{F}} = -\delta_d \hat{\mathcal{F}} + \frac{\Omega_f}{2}\hat{\mathcal{P}} \tag{S6}$$

We now make the approximation of adiabatically eliminating the intermediate-state excitation $\hat{\mathcal{P}}$ by setting its time-derivative to zero. While this is typically justified when $|\Delta| \gg \Omega_r, \Omega_f$, we have found this to be a good approximation even in the $|\Delta| \sim \Omega_r, \Omega_f$ regime, as verified by comparing numerical simulations of two-particle problem with the full set of equations and that with $\hat{\mathcal{P}}$ adiabatically eliminated. We obtain:

$$i\partial_t \hat{\mathcal{E}} = -ic\partial_z \hat{\mathcal{E}} + \frac{g^2}{4\Delta}\hat{\mathcal{E}} + \frac{g\Omega_r}{4\Delta}\hat{\mathcal{R}} + \frac{g\Omega_f}{4\Delta}\hat{\mathcal{F}} \tag{S7}$$

$$i\partial_t \hat{\mathcal{R}} = -\delta_r \hat{\mathcal{R}} + \frac{g\Omega_r}{4\Delta}\hat{\mathcal{E}} + \frac{\Omega_r^2}{4\Delta}\hat{\mathcal{R}} + \frac{\Omega_r\Omega_f}{4\Delta}\hat{\mathcal{F}} + \int dz' V(z-z')\hat{\mathcal{R}}^\dagger(z')\hat{\mathcal{R}}(z')\hat{\mathcal{R}}(z) \tag{S8}$$

$$i\partial_t \hat{\mathcal{F}} = -\delta_f \hat{\mathcal{F}} + \frac{g\Omega_f}{4\Delta}\hat{\mathcal{E}} + \frac{\Omega_f^2}{4\Delta}\hat{\mathcal{F}} + \frac{\Omega_r\Omega_f}{4\Delta}\hat{\mathcal{R}} \tag{S9}$$

This indicates that the effective Hamiltonian under this approximation is $\mathcal{H}' = \mathcal{H}_0' + \mathcal{H}_{\text{int}}$

$$\mathcal{H}_0' = \mathcal{H}_0 = \int dz \begin{pmatrix} \hat{\mathcal{E}} \\ \hat{\mathcal{R}} \\ \hat{\mathcal{F}} \end{pmatrix}^\dagger \begin{pmatrix} -ic\partial_z + g^2/4\Delta & g\Omega_r/4\Delta & g\Omega_f/4\Delta \\ g\Omega_r/4\Delta & -\delta_r + \Omega_r^2/4\Delta & \Omega_r\Omega_f/4\Delta \\ g\Omega_f/2 & \Omega_r\Omega_f/4\Delta & -\delta_f + \Omega_f^2/4\Delta \end{pmatrix} \begin{pmatrix} \hat{\mathcal{E}} \\ \hat{\mathcal{R}} \\ \hat{\mathcal{F}} \end{pmatrix} \tag{S10}$$

which we will use for the remainder of the derivation.

A. Single-particle dynamics

Let us first look at a single particle case, for which the wavefunction takes the form

$$|\psi\rangle = \int dz \sum_{A\in\{E,R,F\}} A(z,t)\hat{\mathcal{A}}^\dagger(z)|0\rangle \tag{S11}$$

We perform the following transformation on the coefficients:

$$A(z,t) = \sum_{k,\omega} A(k,\omega)e^{i(k+k_0)z - i\omega t} \quad \text{where} \quad k_0 = \frac{-g^2\delta_r\delta_f}{c\Gamma_1} \quad \text{and} \quad \Gamma_1 = 4\delta_r\delta_f\left(\Delta - \frac{\Omega_r^2}{4\delta_r} - \frac{\Omega_f^2}{4\delta_f}\right) \tag{S12}$$

The added momentum shift of k_0 makes it so that in the new momentum-frequency (k,ω) basis, the zero-frequency $(\omega = 0)$ eigenstate is at zero momentum $(k = 0)$. For the single-particle case, we get the following equations of motion for the coefficients:

$$\omega E = \big(\frac{g^2}{4\Delta} + k_0 c + kc\big)E + \frac{g\Omega_r}{4\Delta}R + \frac{g\Omega_f}{4\Delta}F \tag{S13}$$

$$\omega R = -\delta_r R + \frac{g\Omega_r}{4\Delta}E + \frac{\Omega_r^2}{4\Delta}R + \frac{\Omega_r\Omega_f}{4\Delta}F \tag{S14}$$

$$\omega F = -\delta_f F + \frac{g\Omega_f}{4\Delta}E + \frac{\Omega_f^2}{4\Delta}F + \frac{\Omega_r\Omega_f}{4\Delta}R \tag{S15}$$

Solving k as a function of ω will give us the single-particle dispersion relation for our system (shown in Fig. 1D):

$$k(\omega) = \frac{1}{c}\frac{(4\Delta\omega - g^2)(\delta_f+\omega)(\delta_r+\omega) - \omega\Omega_f^2(\delta_r+\omega) - \omega\Omega_r^2(\delta_f+\omega)}{4\Delta(\delta_f+\omega)(\delta_r+\omega) - \Omega_f^2(\delta_r+\omega) - \Omega_r^2(\delta_f+\omega)} - k_0 \tag{S16}$$

where, as mentioned earlier, $k_0 = -g^2\delta_r\delta_f/c\Gamma_1$ is chosen so that $k(0) = 0$.

We can solve the above equation for ω to obtain eigenvalues $\omega = \omega_i(k)$ as a function of k, where $i = 1,2,3$ corresponds to three allowed values of ω. The constant k_0 was chosen so that at $k = 0$, one of the eigenvalue $\omega_i(0) = 0$. We then identify the eigenstate with $\omega = 0$ as a dark state $|d_0\rangle$ with energy $E_{d_0} = 0$ at $k = 0$. In the limit of large collective atom-photon coupling g, the other two values of $\omega_i(k=0)$ are (to leading order in g)

$$E_{d_1} = -\frac{\delta_f^2\Omega_r^2 + \delta_r^2\Omega_f^2}{\delta_f\Omega_r^2 + \delta_r\Omega_f^2} + O(g^{-2}), \quad E_b = \frac{g^2}{4\Delta} + k_0 c + O(g^0), \tag{S17}$$

We note that $E_b \gg E_{d_1}$, and identify the corresponding eigenstates $|b\rangle$ as a bright state and $|d_1\rangle$ as another dark state.

These eigenstates can be smoothly continued as a function of k to obtain eigenstates $|d_{0k}\rangle$, $|d_{1k}\rangle$, and $|b_k\rangle$. This gives rise to the momentum dependence of the dark and bright state energies, from which we can calculate their group velocities and effective masses (at zero-momentum) as defined by

$$v = \frac{\partial\omega}{\partial k}\Big|_{k\to 0} \quad \text{and} \quad m^{-1} = \frac{\partial^2\omega}{\partial k^2}\Big|_{k\to 0} \tag{S18}$$

The expressions for the group velocities of the three states are written below (to leading order in g):

$$v_{d0} = \frac{c\Gamma_1^2}{g^2(\delta_f^2\Omega_r^2 + \delta_r^2\Omega_f^2)} + O(g^{-4}), \quad , v_{d1} = v_{d0}\alpha_x^2 + O(g^{-4}), \quad v_b = c + O(g^{-2}), \tag{S19}$$

where

$$\alpha_x = \frac{\Omega_r\Omega_f(\delta_r - \delta_f)}{\delta_f\Omega_r^2 + \delta_r\Omega_f^2}, \tag{S20}$$

Although the expressions for E_i and v_i are given approximately above, we can write expressions for the effective masses for the three states exactly in terms of E_i and v_i as:

$$m_{d0}^{-1} = 2\left(\frac{v_{d0}v_{d1}}{0 - E_{d1}} + \frac{v_{d0}v_b}{0 - E_b}\right), \quad m_{d1}^{-1} = 2\left(\frac{v_{d1}v_{d0}}{E_{d1} - 0} + \frac{v_{d1}v_b}{E_{d1} - E_b}\right), \quad m_b^{-1} = 2\left(\frac{v_b v_{d0}}{E_b - 0} + \frac{v_b v_{d1}}{E_b - E_{d1}}\right). \tag{S21}$$

B. Two-particle dynamics

In general, the two-particle dynamics for 4-level systems is described by a 16-component system of differential equations. As we have adiabatically eliminated the intermediate-state excitation $\hat{\mathcal{P}}$, we are left with an effective 3-level system with a 9-component system of equations. At the end of the section, we will arrive at a 2-component effective theory written in Eq. (S53) that describes the physics of the 16-component system in steady state limit, with some approximations that we will elaborate on.

We begin by writing the two-particle wavefunction in the following form:

$$|\psi\rangle = \int dz_1 dz_2 e^{ik_0(z_1+z_2)}\left[\sum_{A<B} AB(z_1,z_2,t)\hat{\mathcal{A}}^\dagger(z_1)\hat{\mathcal{B}}^\dagger(z_2) + \frac{1}{2}\sum_A AA(z_1,z_2,t)\hat{\mathcal{A}}^\dagger(z_1)\hat{\mathcal{A}}^\dagger(z_2)\right]|0\rangle \tag{S22}$$

Analogous to the single-particle case, the factor of $e^{ik_0(z_1+z_2)}$ is introduced so that in the non-interacting limit ($V = 0$), there is a zero-energy eigenstate at $k_1 = k_2 = 0$. In addition, we may assume without loss of generality that $AA(z_1, z_2, t) = AA(z_2, z_1, t)$ is symmetric in the two spatial coordinates due to the canonical commutation relation of the bosonic operators. To write down the two-particle equations of motion, it is convenient to switch to the center of mass Z and relative coordinates z:

$$Z = \frac{1}{2}(z_1 + z_2), \quad z = z_2 - z_1 \tag{S23}$$

$$\partial_Z = \partial_{z_1} + \partial_{z_2}, \quad \partial_z = \frac{1}{2}(\partial_{z_2} - \partial_{z_1}) \tag{S24}$$

It is also convenient to define $ER_\pm \equiv ER \pm RE$, $EF_\pm \equiv EF \pm FE$, and $RF_\pm \equiv RF \pm FR$. Note the identity

$$\partial_{z_1}AB \pm \partial_{z_2}BA = \frac{1}{2}\partial_Z AB_\pm - \partial_z AB_\mp. \tag{S25}$$

We then get the following two-particle equations of motion:

$$i\partial_t EE = \left[-ic\partial_Z + 2k_0c + \frac{g^2}{2\Delta}\right]EE + \frac{g\Omega_r}{4\Delta}ER_+ + \frac{g\Omega_f}{4\Delta}EF_+ \tag{S26}$$

$$i\partial_t RR = \left[V(z) - 2\delta_r + \frac{2\Omega_r^2}{4\Delta}\right]RR + \frac{g\Omega_r}{4\Delta}ER_+ + \frac{\Omega_r\Omega_f}{4\Delta}RF_+ \tag{S27}$$

$$i\partial_t FF = \left[-2\delta_f + \frac{\Omega_f^2}{2\Delta}\right]FF + \frac{g\Omega_f}{4\Delta}EF_+ + \frac{\Omega_r\Omega_f}{4\Delta}RF_+ \tag{S28}$$

$$i\partial_t RF_+ = \left[\frac{\Omega_r^2+\Omega_f^2}{4\Delta} - (\delta_r+\delta_f)\right] RF_+ + \frac{g\Omega_r}{4\Delta}EF_+ + \frac{g\Omega_f}{4\Delta}ER_+ + \frac{2\Omega_r\Omega_f}{4\Delta}(FF+RR) \tag{S29}$$

$$i\partial_t RF_- = \left[\frac{\Omega_r^2+\Omega_f^2}{4\Delta} - (\delta_r+\delta_f)\right] RF_- + \frac{g\Omega_r}{4\Delta}EF_- - \frac{g\Omega_f}{4\Delta}ER_- \tag{S30}$$

$$i\partial_t ER_+ = \left[-i\frac{c}{2}\partial_Z + k_0c - \delta_r + \frac{\Omega_r^2}{4\Delta} + \frac{g^2}{4\Delta}\right] ER_+ + ic\partial_z ER_- + \frac{g\Omega_r}{2\Delta}(RR+EE) + \frac{g\Omega_f}{4\Delta}RF_+ + \frac{\Omega_r\Omega_f}{4\Delta}EF_+ \tag{S31}$$

$$i\partial_t EF_+ = \left[-i\frac{c}{2}\partial_Z + k_0c - \delta_f + \frac{\Omega_f^2}{4\Delta} + \frac{g^2}{4\Delta}\right] EF_+ + ic\partial_z EF_- + \frac{g\Omega_f}{2\Delta}(FF+EE) + \frac{\Omega_r\Omega_f}{4\Delta}ER_+ + \frac{g\Omega_r}{4\Delta}RF_+ \tag{S32}$$

$$i\partial_t ER_- = \left[-i\frac{c}{2}\partial_Z + k_0c - \delta_r + \frac{\Omega_r^2}{4\Delta} + \frac{g^2}{4\Delta}\right] ER_- + ic\partial_z ER_+ - \frac{g\Omega_f}{4\Delta}RF_- + \frac{\Omega_r\Omega_f}{4\Delta}EF_- \tag{S33}$$

$$i\partial_t EF_- = \left[-i\frac{c}{2}\partial_Z + k_0c - \delta_f + \frac{\Omega_f^2}{4\Delta} + \frac{g^2}{4\Delta}\right] EF_- + ic\partial_z EF_+ + \frac{g\Omega_r}{4\Delta}RF_- + \frac{\Omega_r\Omega_f}{4\Delta}ER_- \tag{S34}$$

a. Solving for (EE, RR, FF, RF_+, RF_-) — We will first take the steady state limit by setting $\partial_t = 0$.

In the large g limit, the "energy" term of EE, $g^2/2\Delta + 2k_0c$, is large compared to the rest, which allows us to make the approximation that $\partial_Z EE = 0$, analogous to adiabatic elimination. We have verified the validity of this approximation by looking at numerical solutions of these differential equations with and without the $\partial_Z EE = 0$ assumption, and finding them to agree qualitatively.

With these simplifications, we can use Eqs. (S26)-(S30) to express EE, RR, FF, RF_+, RF_- in terms of ER_+, ER_-, EF_+, EF_-. We can then reduce Eqs. (S31)-(S34) to

$$\frac{ic}{2}\partial_Z \begin{pmatrix}\psi_+\\ \psi_-\end{pmatrix} - ic\begin{pmatrix}0 & \mathbb{1}\\ \mathbb{1} & 0\end{pmatrix}\partial_z\begin{pmatrix}\psi_+\\ \psi_-\end{pmatrix} = \left[\begin{pmatrix}H_{0+} & 0\\ 0 & H_{0-}\end{pmatrix} + \begin{pmatrix}H_{V+} & 0\\ 0 & 0\end{pmatrix}\tilde{V}(r)\right]\begin{pmatrix}\psi_+\\ \psi_-\end{pmatrix}, \tag{S35}$$

where ψ_+, ψ_- are

$$\psi_+ = \begin{pmatrix}ER_+(Z,z)\\ EF_+(Z,z)\end{pmatrix}, \qquad \psi_- = \begin{pmatrix}ER_-(Z,z)\\ EF_-(Z,z)\end{pmatrix}. \tag{S36}$$

For the non-interacting part, we have

$$H_{0+} = J_0\delta_r^2\delta_f^2\begin{pmatrix}\Omega_f^2/\delta_f^2 & -(\Omega_r/\delta_r)(\Omega_f/\delta_f)\\ -(\Omega_r/\delta_r)(\Omega_f/\delta_f) & \Omega_r^2/\delta_r^2\end{pmatrix}, \tag{S37}$$

where

$$J_0 \equiv \frac{g^2}{\Gamma_1\Gamma_2} - \frac{1}{\delta_f\Omega_r^2+\delta_r\Omega_f^2}, \quad \Gamma_2 = -4\Delta\left[\delta_r+\delta_f - \frac{\Omega_r^2+\Omega_f^2}{4\Delta}\right], \quad \Gamma_1 = 4\delta_r\delta_f\left(\Delta - \frac{\Omega_r^2}{4\delta_r} - \frac{\Omega_f^2}{4\delta_f}\right). \tag{S38}$$

and

$$H_{0-} = \frac{1}{2}\left[\left(\frac{g^2}{\Gamma_2}+1\right)\frac{\Omega_r^2-\Omega_f^2}{4\Delta} + \delta_f - \delta_r\right]\sigma_z + \left(\frac{g^2}{\Gamma_2}+1\right)\frac{\Omega_r\Omega_f}{8\Delta}\sigma_x + C_{0-}\mathbb{1} \tag{S39}$$

$$\text{where} \quad C_{0-} = \frac{g^2}{2}\left(\frac{1}{4\Delta} - \frac{\delta_r+\delta_f}{\Gamma_2}\right) + \frac{\Gamma_2}{8\Delta} + k_0c. \tag{S40}$$

For the interacting part, we have

$$H_{V+} = \begin{pmatrix}\alpha_{1v} & \alpha_{2v}\\ \alpha_{2v} & \alpha_{5v}\end{pmatrix}, \quad \tilde{V}(z) = \frac{V(z)}{1+V(z)/V_0} \tag{S41}$$

where

$$V_0 = \frac{2\Gamma_1\Gamma_2}{4\Delta\Gamma_1 + (4\Delta\delta_f - \Omega_f^2)^2} \tag{S42}$$

and

$$\alpha_{1v} = \frac{g^2\Omega_r^2(\delta_f\Gamma_2+\delta_r\Omega_f^2)^2}{2\Gamma_1^2\Gamma_2^2}, \quad \alpha_{2v} = \frac{-g^2\delta_f\Omega_r^3\Omega_f(\delta_f\Gamma_2+\delta_r\Omega_f^2)}{2\Gamma_1^2\Gamma_2^2}, \quad \alpha_{5v} = \frac{g^2\delta_f^2\Omega_r^4\Omega_f^2}{2\Gamma_1^2\Gamma_2^2} \tag{S43}$$

b. Eliminating ER_- and EF_- to get two-component theory — In the large g limit, using the parameters we usually work with, the diagonal terms of H_{0-} are much larger than H_{0+}. This allows us to further make the approximation that $\partial_Z \psi_- = 0$, similar to adiabatic elimination. With this approximation, Eq. (S35) reduces to the Hermitian two-component equation:

$$\frac{ic}{2}\partial_Z \psi_+(Z,z) - c^2 H_{0-}^{-1}\partial_z^2 \psi_+(Z,z) = \left[H_{0+} + H_{V+}\tilde{V}(z)\right]\psi_+(Z,z), \tag{S44}$$

We are now very close to the final form of our two-component effective theory. To move further, we note that from Eq. (S26), under the approximation of setting $\partial_Z EE = 0$ and $\partial_t EE = 0$ as we have done earlier, we can write EE as

$$EE = \frac{g/(4\Delta)}{-2(g^2/(4\Delta) + k_0 c)}(\Omega_r ER_+ + \Omega_f EF_+) \tag{S45}$$

Thus, we believe that it will be suggestive to transform the basis of ER_+ and EF_+ using the rotation matrix

$$U = \frac{g/(4\Delta)}{-2(g^2/(4\Delta) + k_0 c)}\begin{pmatrix} \Omega_r & \Omega_f \\ -\Omega_f & \Omega_r \end{pmatrix}, \tag{S46}$$

Using this transformation, we define

$$\boldsymbol{\psi}(Z,z) = U\psi_+(Z,z), \tag{S47}$$

giving

$$\boldsymbol{\psi}(Z,z) = \begin{pmatrix} EE(Z,z) \\ \frac{\Gamma_1}{2g(\delta_f\Omega_r^2 + \delta_r\Omega_f^2)}(-\Omega_f ER_+(Z,z) + \Omega_r EF_+(Z,z)) \end{pmatrix} \equiv \begin{pmatrix} \psi_1(Z,z) \\ \psi_2(Z,z) \end{pmatrix} \tag{S48}$$

Conveniently, we find that in the large g limit, U approximately diagonalizes H_{0-} (see Eq. (S39)):

$$\overleftrightarrow{M}^{-1} = -2v_{\mathrm{avg}}(UH_{0-}^{-1}U^{-1}) \approx \begin{pmatrix} \frac{1}{2m_{\mathrm{EE}}} & 0 \\ 0 & \frac{1}{2m_2} \end{pmatrix} + O(g^{-6}), \tag{S49}$$

where

$$v_{\mathrm{avg}} = \frac{v_{d0} + v_{d1}}{2}, \quad m_{\mathrm{EE}} = \frac{m_{d0}m_{d1}}{m_{d0} + m_{d1}}, \quad m_2 = \frac{-g^4(\delta_f\Omega_r^2 + \delta_r\Omega_f^2)^2(\delta_f^2\Omega_r^2 + \delta_r^2\Omega_f^2)}{2c^2(\Omega_r^2 + \Omega_f^2)\Gamma_2\Gamma_1^3}. \tag{S50}$$

We now describe the remaining expressions in our two-component equation of Eq. (S53) in the rotated basis:

$$\overleftrightarrow{E}_0 = \frac{2v_{\mathrm{avg}}}{c}(UH_{0+}U^{-1}) \approx \frac{\Gamma_1}{\Gamma_2}\begin{pmatrix} \alpha_x^2 & -\alpha_x \\ -\alpha_x & 1 \end{pmatrix} + O(g^{-2}) \tag{S51}$$

$$\overleftrightarrow{E}_v = \frac{2v_{\mathrm{avg}}}{c}(UH_{v+}U^{-1}) \approx \frac{\Omega_r^2}{2\Gamma_2^2(\delta_f\Omega_r^2 + \delta_r\Omega_f^2)^2}$$
$$\begin{pmatrix} \Omega_r^2(\Gamma_1 + 4\Delta\delta_f^2)^2 & -\Omega_r\Omega_f(\Gamma_1 + 4\Delta\delta_f^2)((\delta_r + \delta_f)(4\Delta\delta_f - \Omega_f^2) - 2\delta_f\Omega_r^2) \\ -\Omega_r\Omega_f(\Gamma_1 + 4\Delta\delta_f^2)((\delta_r + \delta_f)(4\Delta\delta_f - \Omega_f^2) - 2\delta_f\Omega_r^2) & \Omega_f^2((\delta_r + \delta_f)(4\Delta\delta_f - \Omega_f^2) - 2\delta_f\Omega_r^2)^2 \end{pmatrix}$$
$$+ O(g^{-2}) \tag{S52}$$

The effective two-particle dynamics in our system can be then described by the following two-component Schrödinger equation:

$$\boxed{iv_{\mathrm{avg}}\partial_Z \boldsymbol{\psi}(Z,z) = -\overleftrightarrow{M}^{-1}\partial_z^2\boldsymbol{\psi}(Z,z) + (\overleftrightarrow{E}_0 + \overleftrightarrow{E}_v\tilde{V}(z))\boldsymbol{\psi}(Z,z),} \tag{S53}$$

This equation holds when our approximations hold, which we summarize here:

- intermediate-state excitation $\hat{\mathcal{P}}$ can be adiabatically eliminated
- steady state limit by setting all time-derivatives to zero: $\partial_t = 0$
- $\partial_Z EE = \partial_Z ER_- = \partial_Z EF_- = 0$

C. Comparing full theory with two-component effective theory

The simulations in the main text are carried out using the full two-particle equations of motion (S26)-(S34). The approximations used to derive the effective two component equation (S53) makes quantitative comparisons with experiment difficult, but as discussed in the main text equation (S53) can provide insight into why we obtain repulsion and attraction between photons. In order to compare the full set of two-particle equations and the effective theory, we compare the simulation results of both over several values of single-photon detuning Δ and two-photon detuning to the Rydberg state δ_r. We identify regions of repulsion, attraction, positive phase, and negative phase show in Figure S1. The good agreement between the two simulations in identifying the right features implies that we can use equation (S53) as a predictor for the nature of interactions between two photons.

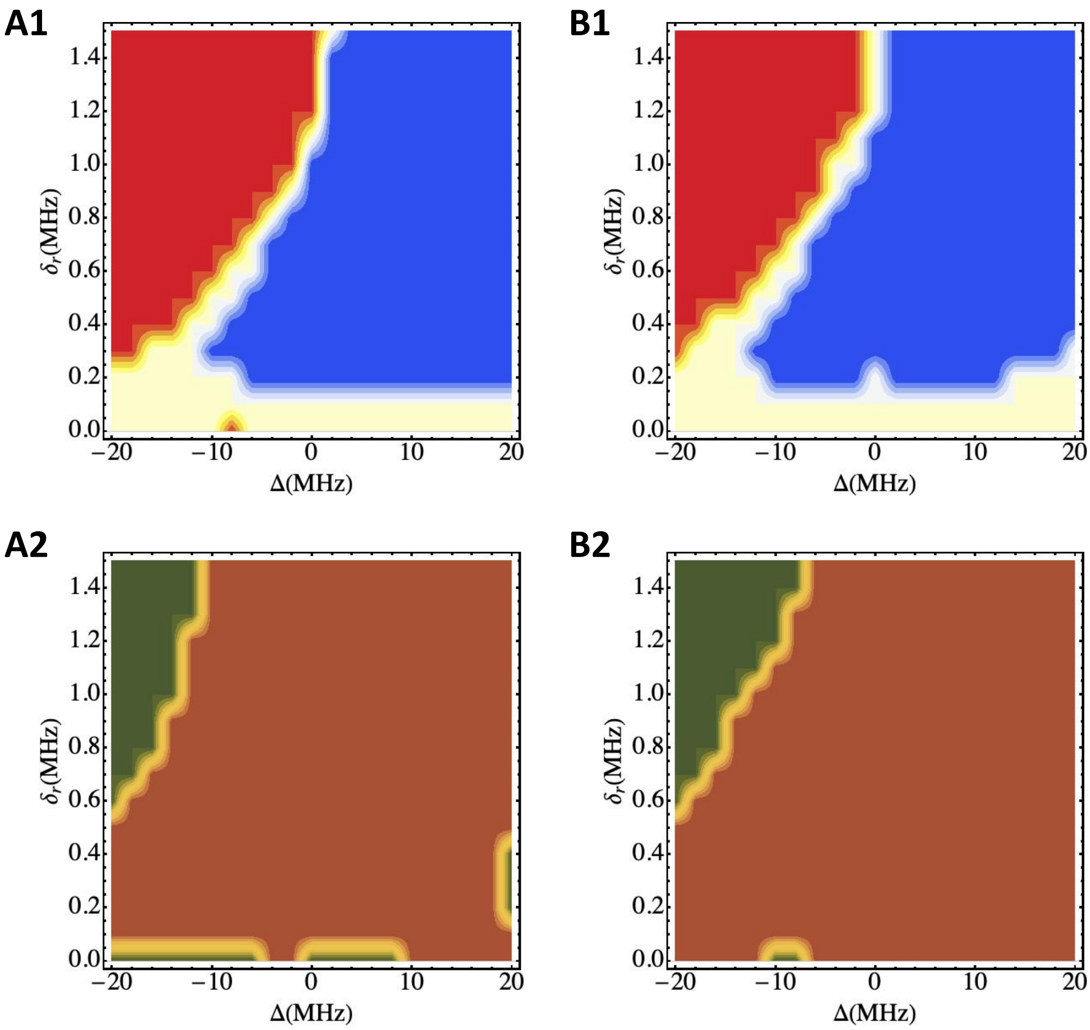

FIG. S1: **Comparing full numerics with effective theory. A1, B1** Comparing regions of effective interaction - red corresponds to repulsion, blue corresponds to attraction, and yellow corresponds to dissipation/ no correlation. **A1** is the result from the full numerics and **B1** is the result of simulating the effective theory. Repulsion is characterized by antibunching $g^2(0) < 0.95$ followed by bunching at a later time $g^2(\tau_R) > 1.05$. Attraction is characterized by the bunching $g^2(0) > 1.05$ and all other cases are characterized by dissipation or have no correlation. **A2, B2** Comparing sign of two photon phase - green is positive phase $\phi^2(0)$ and brown is negative phase $\phi^2(0)$. **A2** is the result from the full numerics and **B2** is the result of simulating the effective theory. Both simulations are carried out at parameters - $\Omega_r = 20$ MHz and $\Omega_f = 12$ MHz, $\delta_f = -\delta_r$.